



OPEN Whitening efficacy and enamel properties of 30% hydrogen peroxide solution incorporated with strontium-containing Fluorapatite

Ji-Yeon Hong^{1,2}, Eo-Jin Kang^{1,2} & Jae-Sung Kwon^{1,2}✉

This study evaluated the effects of 30% hydrogen peroxide (HP) solution incorporated with strontium-containing Fluorapatite (Sr-FAp) on whitening efficacy and enamel surface properties, aiming to minimize enamel damage during bleaching. A total of 60 extracted bovine teeth were stained with black tea and divided into five groups ($n = 12$): DW (distilled water), 30% HP, 1 wt% Sr-FAp + HP, 5 wt% Sr-FAp + HP, and 10 wt% Sr-FAp + HP. DW and HP solutions with or without Sr-FAp were applied three times for 20 min each. The surface color alteration, gloss, roughness, microhardness, and enamel microstructure were analyzed before and after bleaching. All experimental groups showed significantly higher ΔE_{ab} values than those of the DW group ($p < 0.05$), with no significant differences between Sr-FAp concentrations ($p > 0.05$). ΔWID and ΔE_{00} followed similar trends. Gloss decreased in all HP-treated groups compared to the DW group ($p < 0.05$), with the 10 wt% Sr-FAp group showing the lowest gloss ($p < 0.05$). There were no significant differences in surface roughness ($p > 0.05$), whereas the 10 wt% Sr-FAp group showed the highest microhardness value ($p < 0.05$). Observations of the enamel surface revealed the presence of Sr-FAp nanoparticles in all Sr-FAp groups. HP containing Sr-FAp effectively whitened the teeth while preserving the enamel microhardness and structure via a protective Sr-FAp layer. Sr-FAp shows promise as a remineralizing filler for whitening treatments, maintaining whitening efficacy while minimizing enamel damage.

Keywords Tooth whitening treatment, 30% hydrogen peroxide, Hydroxyapatite, Strontium-containing fluorapatite (Sr-FAp), Bleaching efficacy, Enamel properties

Tooth whitening treatments have become one of the most commonly performed aesthetic procedures in dentistry¹ owing to their ease of application, proven efficacy, and safety, particularly given the increasing emphasis on aesthetics². Hydrogen peroxide (HP) is commonly used as a tooth bleaching agent to generate free radicals that oxidize the stained organic molecules³. In-office bleaching is dental treatment widely used for its excellent whitening efficacy, achieved by applying high concentration of 30–40% HP for a short period of time⁴. However, various side effects can arise from the use of high HP concentrations. For example, they have been observed to cause calcium loss on the enamel surface^{5–7}. In addition, many studies have reported several side effects such as surface morphology changes⁸, alterations in chemical composition^{7,9–11} and reduction of enamel microhardness¹². Thus, efforts are needed to reduce the side effects that may occur due to the high concentrations of HP.

Hydroxyapatite (HAp, $\text{Ca}_{10}(\text{PO}_4)_6(\text{OH})_2$) has chemical and structural similarities to human's teeth^{13,14}. HAp is a substance widely used in dentistry for blocking dentinal tubules and promoting remineralization^{15,16}. A previous study demonstrated that adding HAp to 35% HP forms a protective layer, protecting against oxidative damage caused by high-concentration HP¹⁷. These materials saturate enamel surfaces with calcium and phosphate ions, reduce enamel demineralization during bleaching and act as a physical barrier^{15,16}. Despite its various optimal properties, poor mechanical properties and chemical stability of HAp limit its clinical applications¹⁸. Research on improving the properties of HAp through substitution has been actively conducted

¹Department and Research Institute of Dental Biomaterials and Bioengineering, Yonsei University College of Dentistry, 50-1 Yonsei-ro, Seodaemun-gu, Seoul 03722, Republic of Korea. ²BK21 FOUR Project, Yonsei University College of Dentistry, Seoul, Korea. ✉email: jkwon@yuhs.ac

in recent years, as several ionic substitutions are present in biological apatites, each of which play an important role in their overall biological performance, such as bioactivity, biocompatibility, and solubility¹⁹.

Strontium-containing Fluorapatite (Sr-FAp), in which Sr²⁺ substitutes for Ca²⁺ and F⁻ replaces OH⁻²⁰. Sr-FAp has been used as a bone graft material and filler because of its strong remineralization effects^{21,22}. Substituting ions existing in the body's hard tissues, such as strontium and fluoride, into HA can enhance the biomaterial's characteristics, potentially improving its bioactivity^{23,24}. Fluoride is an essential trace element in the human body. When incorporated into the apatite crystal structure, it forms Fluorapatite (FAp, Ca₁₀(PO₄)₆(F)₂) crystals, which have much higher physical and chemical stability, including enhanced resistance to acid dissolution and demineralization. Strontium is a trace element found in bones and teeth with properties similar to those of calcium²⁵. This plays a crucial role in induction of apatite crystal precipitation²⁶. Despite these characteristics, studies on the application of Sr-FAp in HP are limited. To this end, we examine the addition of Sr-FAp with various contents to 30% HP, to maintain the whitening efficacy while protecting enamel surface. This study aimed to evaluate the effect of 30% HP solution containing Sr-FAp on whitening efficacy and its enamel protection capabilities, including the surface color, gloss, roughness, microhardness, and micromorphology after bleaching procedure. The null hypotheses of this study were as follows: (1) The whitening efficacy of 30% HP solution is not affected by the presence of Sr-FAp in different concentrations. (2) There is no significant difference in the surface gloss, roughness, microhardness, and micromorphology of the enamel surface between bleaching with 30% HP solution alone or bleaching with 30% HP solution containing Sr-FAp in different concentrations.

Materials and methods
Synthesis of Sr-FAp

Sr-FAp was synthesized by modifying a previously described hydrothermal method from previous study²⁰. In this study, approximately 50 mol% of calcium was substituted with strontium. All reagents were purchased from Sigma-Aldrich (St. Louis, MO, USA). First, Ca(NO₃)₂·4 H₂O (4.55 g) and Sr(NO₃)₂ (4.03 g) were dissolved in distilled water (DW) and stirred at 90 °C. In a separate beaker, (NH₄)₂HPO₄ (3.02 g) and NH₄F (0.28 g) were dissolved in DW and stirred. The two solutions were mixed in a molar ratio of (Ca²⁺+Sr²⁺):PO₄²⁻:(OH⁻+F⁻) = 10:6:2. During continuous stirring, the pH was immediately adjusted to 11 by adding 25% ammonia solution dropwise. The resulting solution was stirred at 90 °C for 1 h. Subsequently, the solution was transferred to a hydrothermal Teflon mold (Hydrothermal Synthesis Autoclave Reactor Vessel Set with PTFE Inner, SciLab[®], Seoul, Korea) and subjected to heat and pressure in a furnace (Lindberg/Blue M[™] Moldatherm[™] Box Furnace, Germany) at 160 °C for 12 h. Subsequently, the product was washed several times with DW, filtered, and dried completely in an oven at 100 °C for 24 h.

Characterization of Sr-FAp

The crystal phases were characterized using X-ray diffraction (XRD, Rigaku Ultima IV X-ray Diffractometer, Tokyo, Japan). To analyze the elemental composition and microstructure of the particles, field emission scanning electron microscopy (FE-SEM, JSM-7610 F-Plus, JEOL Ltd., Korea) was used. The elemental composition was analyzed using energy dispersive x-ray spectroscopy (EDS) mapping. The samples were observed at 20,000× magnification after applying a platinum (Pt) coating for 100 s. To observe the particle size and crystal morphology, transmission electron microscope (TEM, JEM-F200, JEOL, Ltd., Korea) was measured at a 100 nm scale, and particle size was analyzed using the Image J software.

Preparation of HP solution containing Sr-FAp

Sr-FAp powder was added at concentrations of 1%, 5%, and 10% Sr-FAp to a 30% HP solution (Junsei Chemical Co. Ltd., Tokyo, Japan) and mixed for 10 s using a vortex device (Vortex Mixer VM1, LABTron, Seoul, Korea). The 30% HP solution used in this study is an aqueous solution composed of approximately 70% water. To evaluate the effect of Sr-FAp concentration on the pH of the solution, the pH of each experimental group was measured at 37 ± 1 °C using a pH meter (Orion 4 Star, Thermo Fisher Scientific, Singapore), following calibration with standard buffer solutions at pH 4.01, pH 7.0, and pH 10.01. Based on this preparation, five experimental groups with varying Sr-FAp concentrations were established (Table 1).

Preparation of tooth specimens

A total of 60 sound bovine teeth, without caries, cracks, or discolorations, were used in this study.

The bovine teeth were purchased from a company (TSS, Incheon, Korea) that sells the teeth of slaughtered cows. A micromotor (Strong 230, Saeshin Precision, Daegu, Korea) with a diamond-coated disk (NTI-Kahla GmbH, Kahla, Germany) was used to separate the roots from the crowns. The crowns were embedded in a self-cured acrylic resin (Polycoat EC-304, Aekyung Chemical, Chungnam, Korea), and the enamel surface of the

Group	30% Hydrogen peroxide (HP) solution	Strontium-containing Fluorapatite (Sr-FAp)	pH
DW	-	-	6.7
HP	100.0	0.0	2.8
Sr-FAp 1%	99.0	1.0	3.5
Sr-FAp 5%	95.0	5.0	4.1
Sr-FAp 10%	90.0	10.0	4.5

Table 1. Weight ratio of the Strontium-containing fluorapatite (Sr-FAp) in each group (%).

labial surface was exposed and polished using a polishing machine with 1200–2000 grit silicon carbide paper (Deerfos, Incheon, Korea). The 60 polished teeth were randomly assigned to five groups ($n = 12$ per group). For the SEM observations, the specimens were polished to expose the enamel surface without embedding, and three specimens were prepared for each group. Commercial black tea (Lipton Yellow Label TEA, Lipton, Leningrad, Russia) was used to stain the teeth. The tea was prepared following the manufacturer's instructions by steeping one tea bag in 100 mL of DW at 100 ± 1 °C. After cooling to room temperature, the tea was dispensed into each well of a 6-well plate (Cell Culture Plate, SPL Life Sciences Co. Ltd., Pocheon, Korea) using an auto pipette (Portable pipette-Aid[®] XP Controller, Drummond, USA), ensuring that the enamel surfaces were completely submerged. Staining was conducted for six days, during which the samples were stored in a 37 °C water bath. The staining solution was replaced daily. After staining, the teeth were rinsed with DW for 10 s and air-dried. The dried specimens were placed in a new 6-well plate and stored at room temperature until the experiments were conducted.

Bleaching procedure

The bleaching procedure was performed on the bovine enamel labial surfaces of 12 specimens per group. Before whitening, the Sr-FAp powder corresponding to each experimental group was added to 30% HP solution and mixed using vortex mixer for 10 s to ensure uniform distribution immediately before application. 200 μ L of the mixture was applied to completely cover the enamel labial surface of the stained teeth. DW and HP solution were applied in the same manner. Whitening was performed for 20 min per session, followed by rinsing with DW for 10 s and drying with compressed air. The whitening procedure was repeated thrice, with the experimental solution replaced before each session.

Color measurement of enamel surface

To assess color changes before and after whitening, a spectrophotometer (CM-3500d, Minolta, Osaka, Japan) was used in the specular component excluded (SCE) mode with a 3 mm measurement area. Color measurements were taken before staining, after staining, and after whitening of three randomly selected areas on the enamel surface ($n = 12$ per group). Measurements were conducted according to the standards prescribed by the Commission Internationale de l'Eclairage – CIE (International Commission on Illumination). L^* represents brightness, where 100 indicates white and 0 represents black. The a^* value defines the red-green balance, where positive values indicate a red shift, and negative values indicate a green shift. The b^* value defines the yellow-blue balance, where positive values indicate a yellow shift, and negative values indicate a blue shift. Color differences were quantified using three standard formulas. The total color change was: ΔE_{ab} calculated using the equation: $\Delta E_{ab}^* = [(\Delta L^*)^2 + (\Delta a^*)^2 + (\Delta b^*)^2]^{1/2}$ ²⁷. Additionally, the Whitening Index for Dentistry (ΔWI_D) was determined as follows: $\Delta WI_D = 0.511L^* - 2.324a^* - 1.100b^*$. Finally, color difference according to the CIEDE 2000 system (ΔE_{00}) was calculated using: $E_{00} = [(\Delta L/KL \times SL) + (\Delta C/KC \times SC)^2 + (\Delta H/KH \times SH)^2 + RT \times (\Delta C/KC \times SC) \times (\frac{\Delta H}{KH} \times SH)]^{1/2}$, where ΔL^* , ΔC^* , and ΔH^* represent differences in brightness, chroma, and hue between two samples, respectively. The rotation function (RT) explains the interaction between chroma and hue differences in the blue region. SL, SC, and SH are the weighting functions for the lightness, chroma, and hue components, respectively. KL, KC, and KH are parameter constants that are set to 1²⁸.

Gloss of enamel surface

To determine the Gloss Unit (GU) values, the enamel labial surface was measured using a glossmeter (Novo-Curve Gloss Meter, Rhopoint Instruments, East Sussex, UK) after both staining and whitening ($n = 12$ per group). Prior to gloss measurement, calibration was performed using a calibration tile. The gloss values were measured in three randomly selected areas on the enamel surface, and the average value was calculated.

Roughness of enamel surface

The surface roughness of the enamel was measured using a 3D optical surface roughness analyzer (Contour GT-X3 BASE, GTX-12-121, Bruker, USA) to assess changes before and after whitening ($n = 12$ per group). The measurement conditions were standardized with scan speed set to 1 \times , a back scan distance of 5 μ m, and a measurement length of 25 μ m. The roughness values, obtained after both staining and whitening, were expressed as Ra values to quantify surface texture variations. Measurements were taken at three randomly selected areas on the enamel surface, and the average value was calculated to ensure accuracy and reproducibility.

Microhardness of enamel surface

The microhardness of the enamel surface was measured using the Vickers hardness test. A DMH-2 hardness tester (Matsuzawa Seiki Co., Tokyo, Japan) was used to perform measurements after staining and whitening ($n = 12$ per group). A load of 200 g was applied for 15 s to create diamond-shaped indentations. The diagonal length of the indentation was measured to calculate the microhardness values. For each experimental group, microhardness was measured in three randomly selected areas on the enamel surface, and the average value was calculated.

SEM-EDS analysis

To analyze the microstructure of the enamel surface, three specimens from each experimental group were treated with a whitening agent ($n = 3$ per group). Prior to the SEM observation, a 100 nm thick Pt coating was applied. Observations were conducted using field-emission scanning electron microscopy (FE-SEM; JSM-7800 F, JEOL

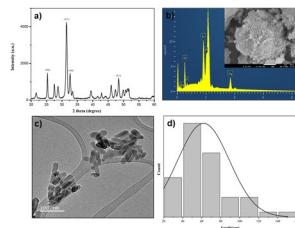


Fig. 1. Characterization of synthesized Sr-FAp. (a) The X-ray diffraction (XRD) pattern, (b) Field-emission scanning electron microscopy (FE-SEM) image and energy dispersive x-ray spectroscopy (EDS) of Sr-FAp, (c) Transmission electron microscope (TEM) for morphology, and (d) Particle size distribution.

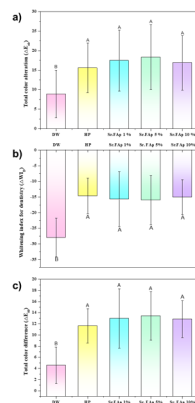


Fig. 2. Mean values of (a) Total color alteration (ΔE_{ab}), (b) Whitening index in dentistry (ΔWI_D), and (c) Total color alteration by CIED 2000 (ΔE_{00}) for each experimental group ($n = 12$). Error bars represent standard deviations (SD). Groups with the same letters are not significantly different ($p > 0.05$).

Ltd., Seoul, Korea) at 2,000 \times and 15,000 \times magnifications. EDS mapping was performed to examine the elemental composition of the particles remaining on the enamel surface.

Statistical analysis

Color change, microhardness, and roughness were analyzed using One-way ANOVA (SPSS27, IBM Co., Armonk, NY, USA). Tukey's post-hoc test was used for further analyses. The significance level was set at $p < 0.05$. An independent samples t-test was performed to compare the values before and after whitening.

Results

Characterization of the Sr-FAp

Figure 1a shows the XRD pattern of the synthesized Sr-FAp. Peaks corresponding to the apatite phase were detected, confirming its formation. This pattern closely resembles that reported in a previous study²². Figure 1b presents an FE-SEM image of Sr-FAp. SEM images revealed that the nano sized particles were aggregated, and EDS mapping at 20,000 \times magnification detected Ca, Sr, P, O, and F ions. Figure 1c shows a TEM image of Sr-FAp, which exhibits a needle like morphology characteristic of apatite structures. Figure 1d shows the particle size distribution analysis using Image J software. The average particle length was 61.9 ± 26.9 nm, with a median length of 51.16 nm.

Color measurements of enamel surface

The ΔE_{ab} , ΔWI_D , and ΔE_{00} values are shown in (Fig. 2). All bleached groups exhibited significantly higher ΔE_{ab} values than those of the DW group ($p < 0.05$) (Fig. 2a). However, within the 30% HP solution, ΔE_{ab} values showed no significant differences regardless of the Sr-FAp content ($p > 0.05$). Similarly, the ΔWI_D results indicated that the DW group had the lowest ΔWI_D values, whereas the all bleached groups exhibited significantly increased ΔWI_D values compared to the DW group ($p < 0.05$) (Fig. 2b). The ΔE_{00} values followed a similar trend, with all bleached groups showing significantly higher color differences compared to the DW group ($p < 0.05$) (Fig. 2c). DW was the only group showing a significantly lower ΔE_{00} ($p > 0.05$).

Gloss of enamel surface

The GU results are shown in Fig. 3a. Before whitening, no significant differences were observed between groups ($p > 0.05$). However, after the whitening procedure, significant differences were observed between the experimental groups ($p < 0.05$). The DW group showed no significant difference before and after whitening

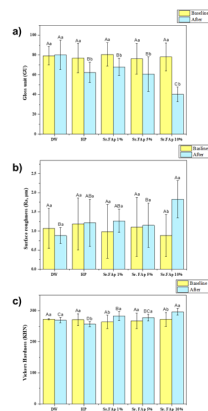


Fig. 3. Mean values of (a) Surface gloss (GU), (b) Roughness (Ra), and (c) Vickers hardness (KHN) at baseline and after bleaching treatment ($n = 12$). Error bars represent the standard deviations (SD). The same uppercase letters indicate no significant differences among the groups at each time point ($p > 0.05$), while the same lowercase letters indicate no significant differences between baseline and after treatment within each group ($p > 0.05$).

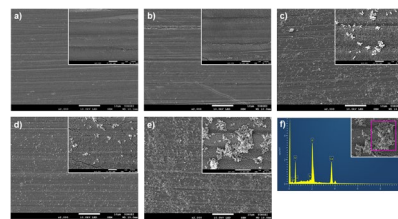


Fig. 4. SEM images of the experimental groups ($n = 3$) with magnifications of 2,000× and 15,000×. Bleaching treatment with (a) DW group, (b) HP group, (c) Sr-FAP 1 wt% group, (d) Sr-FAP 5 wt% group, (e) Sr-FAP 10 wt% group, and (f) the EDS mapping image of the particles on the enamel after bleaching treatment for the Sr-FAP 10 wt% group.

($p > 0.05$). However, the HP group and the groups containing Sr-FAP exhibited a significant decrease in gloss ($p < 0.05$). In the Sr-FAP 1 wt% and 5 wt% groups, no significant differences were observed compared to the HP group ($p > 0.05$). In contrast, the Sr-FAP 10 wt% group exhibited a significantly greater decrease in gloss ($p < 0.05$).

Roughness of enamel surface

The surface roughness results are shown in Fig. 3b. Before whitening, no significant differences in Ra values were observed between the groups ($p > 0.05$). After whitening, statistically significant differences were observed compared with before whitening ($p < 0.05$). However, after whitening, roughness increased in the HP, Sr-FAP 1 wt%, and Sr-FAP 5 wt% groups compared to the DW group, but no significant differences were found among these groups ($p > 0.05$). In contrast, the Sr-FAP 10 wt% group showed a significant increase in Ra values ($p < 0.05$).

Microhardness of enamel surface

The microhardness results are presented in Fig. 3c. Before whitening, no statistically significant differences were observed between the experimental groups ($p > 0.05$). After whitening, a significant decrease in hardness was observed in the HP group ($p < 0.05$), whereas groups containing Sr-FAP exhibited an increasing trend in microhardness. The Sr-FAP 10 wt% group exhibited the highest hardness ($p < 0.05$).

Microscopic analysis of enamel surface (SEM-EDS)

SEM images are shown in Fig. 4, which is an illustration of the enamel surface morphology after treatment. In the DW and HP groups, polishing marks were clearly visible on the enamel surfaces. In contrast, fine particles were observed within the gaps of the polished enamel surface in the groups containing Sr-FAP. Visually, no significant difference in the number of adhered particles was detected between the 1 and 5 wt% Sr-FAP groups. However, the 10 wt% Sr-FAP group exhibited the highest particle deposition on the surface. At 20,000× magnification, nano-sized and aggregated particles were observed between the polished enamel surfaces in the Sr-FAP treated groups, with the 10 wt% Sr-FAP group displaying the most extensive particle attachment. EDS mapping analysis of the observed particles confirmed that their elemental composition corresponded to that of Sr-FAP, with detectable levels of Ca, Sr, P, O, and F.

Discussion

This study examined the whitening efficacy and enamel surface protective effects of adding Sr-FAP to 30% HP. Based on the results of this study, we can prove that the 30% HP solution containing Sr-FAP of various contents has bleaching efficacy and holds promise for preventing tooth demineralization. Thus, the first null hypothesis—that the whitening efficacy of a 30% HP solution is not affected by the presence of Sr-FAP in different concentrations—was accepted. Conversely, the second null hypothesis—that there is no significant difference in the surface gloss, roughness, microhardness, and micromorphology of bovine enamel between bleaching with 30% HP solution alone and with 30% HP solution containing Sr-FAP at different concentrations—was rejected. High concentrations of HP solution exhibit excellent whitening effects but are associated with several side effects. To mitigate these effects, several desensitizing agents have been introduced for pre- and post-bleaching treatments or incorporated into bleaching materials²⁹. In this study, Sr-FAP was incorporated into 30% HP solution as a desensitizing material. Sr-FAP has demonstrated excellent remineralization effects by releasing various ions when used as a bone graft material^{20,30,31} or added as a filler to glass ionomer cement (GIC) produced using the sol-gel method²¹. After synthesizing Sr-FAP, XRD, SEM-EDS, and TEM analysis confirmed that its structure, chemical composition, and morphology were consistent with those of previously reported Sr-FAP^{20–22}. Previous tooth bleaching studies have developed reliable in vitro methods to evaluate the effectiveness of tooth bleaching using reproducible discoloration model³². In this study, black tea was used as the staining agent, and bovine teeth were used as the specimens. Black tea has been shown to be effective in enamel staining and has been widely used as a discoloring solution in many studies on tooth bleaching^{33,34} and thus it was selected as the staining agent in this study. Although bovine teeth exhibit microstructural differences from human teeth, such as in prism arrangement³⁵, however, as they share similar chemical and mechanical properties³⁶ bovine enamel has been widely used as an in vitro model in studies related to tooth bleaching and remineralization^{37,38}. Tooth whitening products contain HP solution as an active agent, glycerin as a carrier, carbopol as a thickening agent, and a number of flavoring agents³⁹. Glycerin and carbopol, the most common carriers of bleaching formulas, may also act as a demineralizing agent⁴⁰. To eliminate this effect, a pure 30% HP solution was used in this study. DW, which did not affect the enamel surface, was used as the control. This approach is consistent with that of previous studies³⁸. The bleaching efficacy of tooth bleaching products can be evaluated using various methods, such as comparative analysis using a standard tooth shade guide, and objective methods, including spectrophotometers, colorimeters, and digital cameras⁴¹. Compared with other devices, the spectrophotometric method based on the CIE-Lab system allows for the quantitative evaluation of color changes and serves as a reliable and objective tool^{42,43}. In this study, the ΔE_{ab} value was calculated to assess the color differences before and after whitening, with the recently proposed CIED 2000 formula⁴⁴ showing high correlation and interchangeability with the ΔE_{ab} ⁴⁵. However, these two color difference formulas alone are not sufficient to evaluate color differences, and the authors suggest using other indexes specifically designed to assess whiteness in dental materials and dental evaluations⁴⁶. Therefore, this study utilized all three formulas proposed in the literature to calculate color difference.

Significant color changes were observed in the Sr-FAP and the HP groups compared with those in the DW group following the whitening procedure (Fig. 2). This color change was considered clinically perceptible to the naked eye, as the ΔE_{ab} values obtained were greater than 3.3⁴⁷. This study confirmed superior color differences after whitening in the HP and Sr-FAP containing groups, with similar tendencies in color changes observed across all three formulas (ΔE_{ab} , ΔWI_D , ΔE_{00}). Gruba AS et al. reported similar trends to this study, showing excellent whitening effects with ΔE_{ab} , ΔWI_D , and ΔE_{00} without significant difference compared to HP⁴⁸. This study demonstrated that HP with added Sr-FAP is effective for whitening, and that varying concentrations of Sr-FAP do not affect whitening efficacy. Gloss is an optical phenomenon observed when evaluating the appearance of a surface. The evaluation of gloss describes the capacity of a surface to reflect directed light⁴⁹. In this study, gloss of the enamel surface was observed after treatment in the experimental groups (Fig. 3). Whitening treatment affected the gloss results in all groups except the DW group. GU values did not change before and after treatment in the DW-treated group. In contrast, the GU value significantly decreased regardless of the Sr-FAP content, with the 10 wt% Sr-FAP group showing the lowest GU value. The decrease in gloss is related to the amount of Sr-FAP powder remaining on the enamel surface. The particles observed on the enamel surface in the SEM images were identified as aggregated Sr-FAP powder based on EDS mapping results. Although there was no visually significant difference in the amount of Sr-FAP powder adsorbed on the surface between the Sr-FAP 1 wt% and 5 wt% groups, a noticeably larger number of particles were adsorbed in the Sr-FAP 10 wt% group. Based on the gloss measurements, the Sr-FAP 10 wt% group showed the lowest gloss value, likely due to the adsorption of Sr-FAP powder, which contributed to the reduction in enamel surface gloss. Sr-FAP appears to have acted as a physical protective layer against demineralization during the bleaching process, which may explain its adsorption on the enamel surface observed in the gloss and SEM analyses. A previous study similarly reported that the addition of CPP-ACP to bleaching agents forms a physical barrier on the enamel surface, thereby providing protective effects. This protective layer was also observed on the enamel surface through SEM analysis, confirming its presence and barrier function⁵⁰. Surface roughness refers to the loss of gloss and is key surface property⁵¹. In the results of this study, although there were no significant differences in *Ra* values between groups after the application of the test materials, a significant increase in *Ra* value was observed in the Sr-FAP 10 wt% group. Therefore, it was confirmed that the Sr-FAP 10 wt% group exhibited the lowest gloss and highest roughness values. It was confirmed that the surface roughness increased as the powder adhered, leading to a decrease in gloss. It has been suggested that gloss and roughness can be restored by polishing or tooth brushing after the whitening treatment. The Vickers hardness test is a well established and accurate method for examining the surface properties of human hard dental tissues and dental prostheses^{52–55}. In this study, a significant decrease in microhardness was observed after HP application, indicating enamel demineralization⁵⁶. However, an increase in hardness was observed in the group treated with Sr-FAP, with the 10 wt% group showing

the highest hardness. This suggests that adding 10 wt% Sr-FAP can help reduce the loss of microhardness. As shown in the pH values of each experimental group in Table 1, the HP solution exhibited a strongly acidic pH of 2.8, whereas 10 wt% Sr-FAP had a pH of 4.5, and the overall solution pH increased with higher Sr-FAP content, suggesting that Sr-FAP played a role in neutralizing the acidity, which likely helped minimize enamel demineralization and was accompanied by a corresponding increase in microhardness⁵⁷. Sr-FAP is considered to be adsorbed onto the enamel surface, reducing direct contact between HP and the enamel surface, and serving as a protective layer to prevent demineralization that may occur during the whitening process. Carlos Guilherme Murr et al. demonstrated that two forms of nano sized HAP adhered efficiently to dental enamel, forming a protective layer that minimized direct contact between HP and the enamel surface during dental bleaching, thereby promoting enamel remineralization⁵⁸. The Sr-FAP used in this study was also nano sized, suggesting that effects similar to those observed in previous research can be expected. In addition, ions such as Sr^{2+} , Ca^{2+} , PO_4^{3-} , and F⁻, which constitute Sr-FAP, can be supplied to the enamel surface, providing benefits for remineralization, as shown in Fig. 4. This process can help minimize mineral loss, which is one of the major side effects of tooth whitening. By adhering to the enamel surface during whitening, Sr-FAP can provide a protective effect, while minimizing the major side effects of tooth whitening and mineral loss. Overall, Sr-FAP is a promising material that can be added to HP solutions to protect enamel structure and mitigate the adverse effects of HP solutions on the enamel surface. Among the groups studied, 10 wt% Sr-FAP exhibited the most effective enamel surface protection without compromising whitening efficacy. Therefore, the application of 10 wt% Sr-FAP is highly recommended. The limitation of this study was that only black tea was used, with tannin as the main staining substance. Future studies should investigate whether sufficient whitening efficacy is maintained when various staining solutions are used.

Also, in this study, efforts were made to minimize variability among specimens; however, differences in initial surface roughness (Ra) values were observed between the teeth used. These differences in initial Ra values may have influenced the surface changes observed after treatment. Ideally, analysis based on the before-and-after differences (ΔRa) of each tooth would be preferable. However, due to limitations in the experimental design, this approach could not be fully implemented in the present study. Therefore, variability in initial Ra values should be considered a limitation that may affect the interpretation of the results. Nevertheless, this study is significant as it is the first to examine the effects of various concentrations of Sr-FAP on whitening efficacy and enamel surface characteristics. Sr-FAP added to 30% HP solution not only showed no adverse impact on whitening efficacy but also demonstrated potential by adsorbing to the enamel surface and providing a protective effect. This indicates that Sr-FAP could be used to minimize side effects during the whitening process. Based on these results, our study and results can be used novel bleaching materials.

Conclusions

This study evaluated the effects of a 30% HP solution containing different concentrations of Sr-FAP on tooth whitening efficacy and enamel characteristics following bleaching. The whitening performance of the HP solution was not significantly affected by Sr-FAP concentration. However, significant differences in surface gloss, roughness, microhardness, and micromorphology were varied depending on Sr-FAP content, indicating differences in enamel protection. Notably, the 10% Sr-FAP group demonstrated the most effective protective effect on the enamel without compromising whitening efficacy. Therefore, incorporating 10 wt% Sr-FAP into the bleaching agent may be a promising strategy to minimize enamel damage and demineralization during bleaching.

Data availability

The data will be shared at a reasonable request to J.S.K.

Received: 24 March 2025; Accepted: 2 September 2025

Published online: 06 October 2025

References

1. Fittler, M., Rozmer, Z. & Fittler, A. Rampant online marketing of teeth whitening products: evaluation of online information, labelling accuracy and quantitative analysis of high peroxide content gels. *Heliyon* **9** (2023).
2. VB, H. Current status and recommendations for dentist-prescribed, at-home tooth whitening. *Contemp. Esthet Restor. Pract.* **3**, 2–9 (1999).
3. McEvoy, S. A. Chemical agents for removing intrinsic stains from vital teeth. II. Current techniques and their clinical application. *Quintessence Int.* **20** (1989).
4. Buchalla, W. & Attin, T. External bleaching therapy with activation by heat, light or laser—a systematic review. *Dent. Mater.* **23**, 586–596 (2007).
5. McCracken, M. S. & Haywood, V. B. Demineralization effects of 10% carbamide peroxide. *J. Dent.* **24**, 395–398 (1996).
6. Tezel, H., Ertaş, Ö. S., Özata, F., Dalgat, H. & Korkut, Z. O. Effect of bleaching agents on calcium loss from the enamel surface. *Quintessence Int.* **38** (2007).
7. Al-Salehi, S., Wood, D. & Hatton, P. The effect of 24 h non-stop hydrogen peroxide concentration on bovine enamel and dentine mineral content and microhardness. *J. Dent.* **35**, 845–850 (2007).
8. Bitter, N. C. A scanning electron microscopy study of the effect of bleaching agents on enamel: a preliminary report. *J. Prosthet. Dent.* **67**, 852–855 (1992).
9. Oltu, Ü. & Gürgan, S. Effects of three concentrations of carbamide peroxide on the structure of enamel. *J. Rehabil.* **27**, 332–340 (2000).
10. Cimilli, H. & Pameijer, C. Effect of carbamide peroxide bleaching agents on the physical properties and chemical composition of enamel. *Am. J. Dent.* **14**, 63–66 (2001).
11. Bistey, T., Nagy, I. P., Simó, A. & Hegedűs, C. In vitro FT-IR study of the effects of hydrogen peroxide on superficial tooth enamel. *J. Dent.* **35**, 325–330 (2007).

12. Quintela, S. et al. Silveira de mendonça fragoso, L. Effect of in-office bleaching with 35% hydrogen peroxide with and without addition of calcium on the enamel surface. *Microsc. Res. Tech.* **78**, 975–981 (2015).
13. Dorozhkin, S. V. Calcium orthophosphate-based bioceramics. *Materials* **6**, 3840–3942 (2013).
14. Dorozhkin, S. V. & Epple, M. Biological and medical significance of calcium phosphates. *Angew. Chem. Int. Ed.* **41**, 3130–3146 (2002).
15. Ma, Q., Chen, J., Xu, X. & Wang, T. Impact of transparent tray-based application of bioactive glasses desensitizer on the permeability of enamel and dentin to hydrogen peroxide: an in vitro study. *BMC Oral Health*. **20**, 1–7 (2020).
16. Li, Y., Shi, X. & Li, W. Zinc-containing hydroxyapatite enhances cold-light-activated tooth bleaching treatment in vitro. *BioMed Res. Int.* **2017**, 6261248 (2017).
17. Jiang, T. et al. Beneficial effects of hydroxyapatite on enamel subjected to 30% hydrogen peroxide. *J. Dent.* **36**, 907–914 (2008).
18. Kheradmandfard, M., Fathi, M., Ansari, F. & Ahmadi, T. Effect of Mg content on the bioactivity and biocompatibility of Mg-substituted fluorapatite nanopowders fabricated via mechanical activation. *Mater. Sci. Engineering: C.* **68**, 136–142 (2016).
19. Ahmadi, T. et al. Synthesis and dissolution behavior of nanosized silicon and magnesium co-doped fluorapatite obtained by high energy ball milling. *Ceram. Int.* **40**, 8341–8349 (2014).
20. Wang, Q. et al. Experimental and simulation studies of strontium/fluoride-codoped hydroxyapatite nanoparticles with osteogenic and antibacterial activities. *Colloids Surf., B.* **182**, 110359 (2019).
21. Thongsri, O. et al. Enhanced remineralisation ability and antibacterial properties of sol-gel glass ionomer cement modified by fluoride containing strontium-based bioactive glass or strontium-containing fluorapatite. *Dent. Mater.* **40**, 716–727 (2024).
22. Anastasiou, A. et al. Antibacterial properties and regenerative potential of Sr²⁺ and Ce³⁺ doped fluorapatites; a potential solution for peri-implantitis. *Sci. Rep.* **9**, 14469 (2019).
23. Boanini, E., Gazzano, M. & Bigi, A. Ionic substitutions in calcium phosphates synthesized at low temperature. *Acta Biomater.* **6**, 1882–1894 (2010).
24. Patel, N. et al. A comparative study on the in vivo behavior of hydroxyapatite and silicon substituted hydroxyapatite granules. *J. Mater. Science: Mater. Med.* **13**, 1199–1206 (2002).
25. Guo, D., Xu, K., Zhao, X. & Han, Y. Development of a strontium-containing hydroxyapatite bone cement. *Biomaterials* **26**, 4073–4083 (2005).
26. Albeshti, R. A. *Study on Remineralisation of Glass Ionomer Cements by Solid-State Nuclear Magnetic Resonance Spectroscopy* (2022).
27. International Standard 28399. *2020 Dentistry - External Tooth Bleaching Products*. International Organization for Standardization.
28. Sharma, G., Wu, W. & Dalal, E. N. The CIEDE2000 color-difference formula: implementation notes, supplementary test data, and mathematical observations. Color research & application: endorsed by Inter-Society color council, the colour group (Great Britain), Canadian Society for color, color Science Association of Japan, Dutch Society for the Study of color. *Swed. Colour. Centre Foundation Colour. Soc. Australia Centre Français De La. Couleur.* **30**, 21–30 (2005).
29. Nanjundasetty, J. K. & Ashrafulla, M. Efficacy of desensitizing agents on postoperative sensitivity following an in-office vital tooth bleaching: A randomized controlled clinical trial. *J. Conservative Dentistry Endodontics.* **19**, 207–211 (2016).
30. Anastasiou, A. D. et al. Antibacterial properties and regenerative potential of Sr(2+) and Ce(3+) doped fluorapatites; a potential solution for peri-implantitis. *Sci. Rep.* **9**, 14469 (2019).
31. Kamaei, M. & Fathi, M. H. Preparation and characterization of strontium-fluorapatite nanopowders by sol-gel method. in *AIP Conference Proceedings* (AIP Publishing, 2018). (1920).
32. Sulieman, M., Addy, M. & Rees, J. Development and evaluation of a method in vitro to study the effectiveness of tooth bleaching. *J. Dent.* **31**, 415–422 (2003).
33. Kyaw, K. Y., Otsuki, M., Segarra, M. S. & Tagami, J. Effect of sodium fluoride pretreatment on the efficacy of an in-office bleaching agent: an in vitro study. *Clin. Exp. Dent. Res.* **4**, 113–118 (2018).
34. Yang, S. Y., Choi, J. W., Kim, K. M. & Kwon, J. S. Effects of 35% hydrogen peroxide solution containing hydrated calcium silicate on enamel surface. *Clin. Oral Investig.* 1–10 (2021).
35. Wang, C. et al. The enamel microstructures of bovine mandibular incisors. *Anat. Rec (Hoboken)*. **295**, 1698–1706 (2012).
36. Wang, C. et al. Enamel microstructural features of bovine and human incisors: a comparative study. *Annals Anatomy-Anatomischer Anzeiger.* **235**, 151700 (2021).
37. Alexandrino, L. et al. Effects of a bleaching agent with calcium on bovine enamel. *Eur. J. Dentistry.* **8**, 320–325 (2014).
38. Yang, S. Y., Han, A. R., Kim, K. M. & Kwon, J. S. Effects of incorporating 45S5 bioactive glass into 30% hydrogen peroxide solution on whitening efficacy and enamel surface properties. *Clin. Oral Invest.* **26**, 5301–5312 (2022).
39. Association, A. D. ADA statement on the safety and effectiveness of tooth whitening products. *Retrieved September.* **6**, 2006 (2005).
40. Rodrigues, J. A., Marchi, G. M., Ambrosano, G. M., Heymann, H. O. & Pimenta, L. A. Microhardness evaluation of in situ vital bleaching on human dental enamel using a novel study design. *Dent. Mater.* **21**, 1059–1067 (2005).
41. Lima, D. A. N. L. et al. In vitro evaluation of the effectiveness of bleaching agents activated by different light sources. *J. Prosthodontics: Implant Esthetic Reconstr. Dentistry.* **18**, 249–254 (2009).
42. Joiner, A. The bleaching of teeth: a review of the literature. *J. Dent.* **34**, 412–419 (2006).
43. Dietschi, D., Rossier, S. & Krejci, I. In vitro colorimetric evaluation of the efficacy of various bleaching methods and products. *Quintessence Int.* **37** (2006).
44. Paravina, R. D. et al. Mar Perez, M. D. Color D.fference thresholds in D. ntistry. *J. Esthetic Restor. Dentistry.* **27**, S1–S9 (2015).
45. Alharbi, A., Ardu, S., Bortolotto, T. & Krejci, I. Stain susceptibility of composite and ceramic CAD/CAM blocks versus direct resin composites with different resinous matrices. *Odontology* **105**, 162–169 (2017).
46. Pérez, M. M. et al. Della bona, A. Whiteness difference thresholds in dentistry. *Dent. Mater.* **35**, 292–297 (2019).
47. Vichi, A., Ferrari, M. & Davidson, C. L. Color and opacity variations in three different resin-based composite products after water aging. *Dent. Mater.* **20**, 530–534 (2004).
48. Gruba, A. S. et al. B. Influence of bleaching gels formulated with nano-sized sodium trimetaphosphate and fluoride on the physicochemical, mechanical, and morphological properties of dental enamel. *J. Dent.* **139**, 104743 (2023).
49. Keyf, F. & Etikan, İ. Evaluation of gloss changes of two denture acrylic resin materials in four different beverages. *Dent. Mater.* **20**, 244–251 (2004).
50. Favoreto, M. W. et al. Impact of microabrasion and a remineralizing agent before in-office bleaching on hydrogen peroxide permeability, color alteration, and enamel morphology. *J. Dent.* **156**, 105655 (2025).
51. Alharbi, G., Nahedh, A., Al-Saud, H. N., Shono, L. M., Maawadh, A. & N. & Effect of different finishing and Polishing systems on surface properties of universal single shade resin-based composites. *BMC Oral Health.* **24**, 197 (2024).
52. Meredith, N., Sherriff, M., Setchell, D. & Swanson, S. Measurement of the microhardness and young's modulus of human enamel and dentine using an indentation technique. *Arch. Oral Biol.* **41**, 539–545 (1996).
53. Lippert, F. & Lynch, R. Comparison of Knoop and Vickers surface microhardness and transverse microradiography for the study of early caries lesion formation in human and bovine enamel. *Arch. Oral Biol.* **59**, 704–710 (2014).
54. Kinney, J., Balooch, M., Marshall, S., Marshall Jr, G. & Weihs, T. Hardness and young's modulus of human peritubular and intertubular dentine. *Arch. Oral Biol.* **41**, 9–13 (1996).
55. Omrani, L. R., Khoshamad, S., Ghomshe, E. T., Chiniforush, N. & Kamangar, S. S. H. In vitro effect of bleaching with 810 Nm and 980 Nm diode laser on microhardness of self-cure and light-cure glass ionomer cements. *J. Lasers Med. Sci.* **8**, 191 (2017).
56. Featherstone, J., Ten Cate, J., Shariati, M. & Arends, J. Comparison of artificial caries-like lesions by quantitative microradiography and microhardness profiles. *Caries Res.* **17**, 385–391 (1983).

57. Sun, L. et al. Surface alteration of human tooth enamel subjected to acidic and neutral 30% hydrogen peroxide. *J. Dent.* **39**, 686–692 (2011).
58. Murr, C. G. et al. Synthesis and characterization of different nano-hydroxyapatites and their impact on dental enamel following topical application for dental bleaching. *J. Dent.* **149**, 105291 (2024).

Acknowledgements

This work was supported by the National Research Foundation of Korea (NRF) grant funded by the Korean government (MSIT) (No. 2022R1C1C1010304).

Author contributions

J.Y.H. conceived and designed the experiments. J.Y.H. and E.J.K. performed all the experiments. J.Y.H. interpreted and analyzed the data. J.Y.H. conceived the study and wrote the manuscript. J.S.K. provided manuscript writing assistance and critically revised the manuscript, adding important intellectual content. All authors reviewed and approved the final manuscript.

Declarations

Competing interests

The authors declare no competing interests.

Additional information

Correspondence and requests for materials should be addressed to J.-S.K.

Reprints and permissions information is available at www.nature.com/reprints.

Publisher's note Springer Nature remains neutral with regard to jurisdictional claims in published maps and institutional affiliations.

Open Access This article is licensed under a Creative Commons Attribution-NonCommercial-NoDerivatives 4.0 International License, which permits any non-commercial use, sharing, distribution and reproduction in any medium or format, as long as you give appropriate credit to the original author(s) and the source, provide a link to the Creative Commons licence, and indicate if you modified the licensed material. You do not have permission under this licence to share adapted material derived from this article or parts of it. The images or other third party material in this article are included in the article's Creative Commons licence, unless indicated otherwise in a credit line to the material. If material is not included in the article's Creative Commons licence and your intended use is not permitted by statutory regulation or exceeds the permitted use, you will need to obtain permission directly from the copyright holder. To view a copy of this licence, visit <http://creativecommons.org/licenses/by-nc-nd/4.0/>.

© The Author(s) 2025